

---

# Learning Neural Random Fields with Inclusive Auxiliary Generators

---

**Yunfu Song, Zhijian Ou**  
 Tsinghua University, Beijing, China  
 ozj@tsinghua.edu.cn

## Abstract

In this paper we develop Neural Random Field learning with Inclusive-divergence minimized Auxiliary Generators (NRF-IAG), which is under-appreciated in the literature. The contributions are two-fold. First, we rigorously apply the stochastic approximation algorithm to solve the joint optimization and provide theoretical justification. The new approach of learning NRF-IAG achieves superior unsupervised learning performance competitive with state-of-the-art deep generative models (DGMs) in terms of sample generation quality. Second, semi-supervised learning (SSL) with NRF-IAG gives rise to strong classification results comparable to state-of-art DGM-based SSL methods, and simultaneously achieves superior generation. This is in contrast to the conflict of good classification and good generation, as observed in GAN-based SSL.

## 1 Introduction

One of the core research problems in artificial intelligence is learning with probabilistic models, which could be broadly classified into two classes - directed and undirected<sup>1</sup> [13]. Significant progress has been made recently on learning with deep generative models (DGMs), which generally refer to models with multiple layers of stochastic or deterministic variables, and can be utilized for both unsupervised learning and semi-supervised learning (SSL). Currently, the two most prominent DGM techniques - variational AutoEncoders (VAEs) [12] and generative adversarial networks (GANs) [9], are both directed models. In contrast, undirected generative models (also known as random fields [13], energy-based models [17]), e.g. deep Boltzmann machines (DBMs) [28], received less attention with slow progress. This is presumably because fitting undirected models is more challenging than fitting directed models. In general, calculating the log-likelihood and its gradient is analytically intractable, because this involves evaluating the normalizing constant and, respectively, the expectation with respect to the model distribution.

In this paper, we are interested in learning neural random fields (RFs), particularly those using neural networks with multiple (deterministic) layers to define the potential function<sup>2</sup>. The probability distribution is then defined by normalizing the exponentiated potential function. This type of neural random fields has been studied several times in different contexts. They are once called deep energy models (DEM) in [23, 11], descriptive models in [37], generative ConvNet in [5], neural trans-dimensional random field language models in [33]. In the following, we comment on these related studies and present our two-fold contributions in this paper.

---

<sup>1</sup>An easy way to tell an undirected model from a directed model is that an undirected model involves the normalizing constant (also called the partition function in physics), while the directed model is self-normalized.

<sup>2</sup>Note that compared to modeling with multiple deterministic layers, modeling with multiple stochastic layers presents much greater challenge for model learning and thus yields inferior performance. This is observed in both directed and undirected models.

### 1.1 Related work and our contributions

A recent progress in learning neural random fields as studied in [11, 33, 37] is to pair the target random field with an auxiliary directed generative model (often called generator), which approximates the target random field but is easy to do sampling. Learning is performed by maximizing the target data log-likelihood and simultaneously minimizes some divergence between the target random field and the auxiliary generator. A difference is that [11] minimizes the *exclusive* KL divergence between the target random field and the auxiliary generator, while [33, 37] minimizes the *inclusive* KL divergence. Remarkably, the exclusive divergence includes a reconstruction term and an entropy term, which resembles the expression of the exclusive divergence in the variational learning. The entropy term is analytically intractable, so an ad hoc approximation is used in [11] without strict justification. In contrast, the inclusive divergence does not have such annoying entropy term. Moreover, using inclusive divergence to optimize the auxiliary generator brings additional statistical advantage in model learning due to the asymmetric behaviors of the KL divergences. See discussion in Section 5 after presenting the empirical results.

In this paper we recommend and further develop RF learning with inclusive-divergence minimized auxiliary generators, which is under-appreciated in the literature. [37] provides an intuitive argument that the joint optimization of the target RF and the generator converges to local minima. The issue of using Langevin dynamics without Metropolis-Hastings (MH) accept-reject is overlooked. In this paper, we rigorously apply the stochastic approximation (SA) algorithm [27] to solve the joint optimization and provide theoretical justification. Although [33] uses the SA framework, it uses Metropolis independence sampling (MIS), which is appropriate for discrete data (natural sentences). In contrast, this work handles continuous observations (images) so we propose to utilize SGHMC (stochastic gradient Hamiltonian Monte Carlo) [3] to exploit gradient information with momentum, which is found to perform better than simple Langevin dynamics as used in [37]. The above novelties in RF learning method - rigorous treatment in the SA framework and introducing SGHMC, give the *first contribution* of this paper. The new approach of learning Neural Random Field with Inclusive Auxiliary Generator, abbreviated as NRF-IAG, achieves superior unsupervised learning performance competitive with state-of-the-art DGMs in terms of sample generation quality (as measured by inception score). We also show the capability of NRF-IAGs in latent space interpolation and conditional generation.

Note that different models are needed in unsupervised and semi-supervised learning, because SSL needs to additionally consider labels apart from observations. There are few, if any, priori studies in applying random fields to SSL. The RF model defined for SSL in this paper is novel itself. To the best of our knowledge, this paper is the first demonstration that neural random fields are successfully applied in the challenging SSL tasks. This is the *second contribution* of this paper. Semi-supervised learning of NRF-IAG gives rise to strong classification results comparable to state-of-the-art DGM-based SSL methods, and simultaneously achieves superior generation. This is in contrast to the conflict of good classification and good generation, as observed in GAN-based SSL [29, 7].

There are some studies that connects GANs with energy-based models. The energy-based GAN (EBGAN) model [38], which proposes to view the discriminator as an energy function, is shown to stabilize the training and generate high-resolution images. The further work in [6] aims to address the inability of GANs to provide sensible energy estimates for samples. It connects [38] and [11], and show another two approximations for the entropy term. None of the studies examine their methods or models for SSL, except in EBGAN which performs moderately.

## 2 Background: the SA algorithm

Our method is an application of the stochastic approximation (SA) algorithm [27], which basically provides a mathematical framework for stochastically solving a root finding problem, which has the form of expectations being equal to zeros. Suppose that the objective is to find the solution  $\lambda^*$  of  $f(\lambda) = 0$  with

$$f(\lambda) = E_{z \sim p(\cdot; \lambda)}[F(z; \lambda)], \quad (1)$$

where  $\lambda$  is a  $d$ -dimensional parameter vector in  $\Lambda \subset R^d$ , and  $z$  is an observation from a probability distribution  $p(\cdot; \lambda)$  depending on  $\lambda$ .  $F(z; \lambda) \in R^d$  is a function of  $z$ , providing  $d$ -dimensional noisy

---

**Algorithm 1** Stochastic approximation algorithm with Markov state-dependent noise

---

```

for  $t = 1, 2, \dots$  do
    1. Draw a sample  $z^{(t)}$  with a Markov transition kernel  $K_{\lambda^{(t-1)}}(\cdot | z^{(t-1)})$ , which starts
       with  $z^{(t-1)}$  and admits  $p(\cdot; \lambda^{(t-1)})$  as the invariant distribution.
    2. Set  $\lambda^{(t)} = \lambda^{(t-1)} + \gamma_t F(z^{(t)}; \lambda^{(t-1)})$ , where  $\gamma_t$  is the learning rate.
end for

```

---

measurements of  $f(\lambda)$ . Given some initialization  $\lambda^{(0)}$  and  $z^{(0)}$ , a general SA algorithm iterates as shown in Algorithm 1 [1].

In Algorithm 1,  $F(z^{(t)}; \lambda^{(t-1)}) - f(\lambda^{(t-1)})$ , called the measurement noise, is Markovian state-dependent. The convergence of SA has been studied under various regularity conditions. We provide a short summary of Theorem 5.5 in [1] on the convergence of  $\{\lambda_t, t \geq 1\}$  in the Supplement.

During each SA iteration, it is possible to generate a set of multiple observations  $z$  by performing the Markov transitions repeatedly and then use the average of the corresponding values of  $F(z; \lambda)$  for updating  $\lambda$ , which is known as SA with multiple moves [34]. This technique can help to reduce the fluctuation due to slow-mixing of Markov transitions.

### 3 Learning Neural Random Fields with Inclusive Auxiliary Generators

Consider a random field for modeling observation  $x$  with parameter  $\theta$ :

$$p_\theta(x) = \frac{1}{Z(\theta)} \exp [u_\theta(x)] \quad (2)$$

where  $Z(\theta) = \int \exp(f(x; \theta))dx$  is the normalizing constant,  $u_\theta(x)$  is the potential function<sup>3</sup> which assigns a scalar value to each configuration of random variable  $x$ . The general idea of defining a neural random field is to implement  $u_\theta(x)$  by a neural network, taking  $x$  as input and outputting  $u_\theta(x)$ , so that we can take advantage of the representation power of neural networks<sup>4</sup>. It is usually intractable to maximize the data log-likelihood  $\log p_\theta(\tilde{x})$  for observed  $\tilde{x}$ , since the gradient involves expectation w.r.t. the model distribution, as shown below:

$$\frac{\partial}{\partial \theta} \log p_\theta(\tilde{x}) = \frac{\partial}{\partial \theta} u_\theta(\tilde{x}) - E_{p_\theta(x)} \left[ \frac{\partial}{\partial \theta} u_\theta(x) \right]$$

#### 3.1 Introducing inclusive-divergence minimized auxiliary generators

We provide in Section 1.1 some comparative comments about related previous studies [11, 33, 37] in learning neural random fields. In this paper, we further develop RF learning with inclusive-divergence minimized auxiliary generators<sup>5</sup>. In this paper, we are mainly concerned with modeling fixed-dimensional continuous observations (e.g. images), and choose a directed generative model,  $q_\phi(x, h) \triangleq q(h)q_\phi(x|h)$ , for the auxiliary generator, which is specifically defined as follows<sup>6</sup>:

$$\begin{aligned} h &\sim \mathcal{N}(0, I_h), \\ x &= g_\phi(h) + \epsilon, \epsilon \sim \mathcal{N}(0, \sigma^2 I_\epsilon). \end{aligned} \quad (3)$$

$g_\phi(h)$  is implemented as a neural network with parameter  $\phi$ , which maps the latent code  $h$  to the observation space. Drawing samples from the generator  $q_\phi(x, h)$  is simple as it is just ancestral sampling from a 2-variable directed graphical model.

---

<sup>3</sup>Negating the potential function defines the energy function.

<sup>4</sup>Remarkably, the RFs used in our experiments are different from the neural RFs in previous studies [11, 33, 37]. The differences are: [11] includes linear and squared terms in  $u_\theta(x)$ , [33] defines over sequences, and [37] defines in the form of exponential tilting of a reference distribution (Gaussian white noise).

<sup>5</sup>There exist different choices for the generator, e.g. a GAN model in [11], a LSTM in [33], or a latent-variable model in [37]. All are easy to do sampling.

<sup>6</sup>Note that during training,  $\sigma^2$  is absorbed into the learning rates and does not need to be estimated.

---

**Algorithm 2** Learning neural RFs with inclusive auxiliary generators

---

**repeat**

 Monte Carlo sampling: Draw a unsupervised minibatch  $\mathcal{U} \sim \tilde{p}(\tilde{x})p_\theta(x)q_\phi(h|x)$ ;  
 SA updating:

 Update  $\theta$  by ascending:  $\frac{1}{|\mathcal{U}|} \sum_{(\tilde{x}, x, h) \sim \mathcal{U}} \left[ \frac{\partial}{\partial \theta} u_\theta(\tilde{x}) - \frac{\partial}{\partial \theta} u_\theta(x) \right]$ 

 Update  $\phi$  by ascending:  $\frac{1}{|\mathcal{U}|} \sum_{(\tilde{x}, x, h) \sim \mathcal{U}} \frac{\partial}{\partial \phi} \log q_\phi(x, h)$ 
**until** convergence

---

Suppose that data  $\mathcal{D} = \{\tilde{x}_1, \dots, \tilde{x}_n\}$ , consisting of  $n$  observations, are drawn from the true but unknown data distribution  $p_*(\cdot)$ .  $\tilde{p}(\tilde{x}) \triangleq \frac{1}{n} \sum_{k=1}^n \delta(\tilde{x} - \tilde{x}_k)$  denotes the empirical data distribution. Then we can formulate the maximum likelihood learning as optimizing<sup>7</sup>

$$\begin{cases} \min_{\theta} KL[\tilde{p}(\tilde{x}) || p_\theta(\tilde{x})] \\ \min_{\phi} KL[p_\theta(x) || q_\phi(x)] \end{cases} \quad (4)$$

By setting the gradients to zeros, the above optimization problem can be solved by finding the root for the following system of simultaneous equations:

$$\begin{cases} E_{\tilde{p}(\tilde{x})} \left[ \frac{\partial}{\partial \theta} \log p_\theta(\tilde{x}) \right] = E_{\tilde{p}(\tilde{x})} \left[ \frac{\partial}{\partial \theta} u_\theta(\tilde{x}) \right] - E_{p_\theta(x)} \left[ \frac{\partial}{\partial \theta} u_\theta(x) \right] = 0 \\ E_{p_\theta(x)} \left[ \frac{\partial}{\partial \phi} \log q_\phi(x) \right] = E_{p_\theta(x)q_\phi(h|x)} \left[ \frac{\partial}{\partial \phi} \log q_\phi(x, h) \right] = 0 \end{cases} \quad (5)$$

It can be shown that Eq.(5) exactly follows the form of Eq.(1), so that we can apply the SA algorithm to find its root and thus solve the optimization problem Eq.(4). The SA algorithm with multiple moves is shown in Algorithm 2.

**Proposition 1.** *If Eq.(5) is solvable, then we can apply the SA algorithm to find its root.*

*Proof.* This can be readily shown by recasting Eq.(5) in the form of  $f(\lambda) = 0$ , with  $\lambda \triangleq (\theta, \phi)^T$ ,  $z \triangleq (\tilde{x}, x, h)$ ,  $p(z; \lambda) \triangleq \tilde{p}(\tilde{x})p_\theta(x)q_\phi(h|x)$ , and

$$F(z; \lambda) \triangleq \left( \begin{array}{c} \frac{\partial}{\partial \theta} u_\theta(\tilde{x}) - \frac{\partial}{\partial \theta} u_\theta(x) \\ \frac{\partial}{\partial \phi} \log q_\phi(x, h) \end{array} \right).$$

According to Theorem 2, the SA algorithm converges to a fixed point of Eq.(5).  $\square$

### 3.2 Constructing Markov transition kernel and applying SA rigorously

To apply the SA algorithm, we need to construct a Markov transition kernel  $K_\lambda(\cdot | z^{(t-1)})$  that admits  $p(z; \lambda)$  as the invariant distribution. It is straightforward to draw from  $\tilde{p}(\tilde{x})$ , and the problem is to construct the Markov kernel  $K_{\theta, \phi}(\cdot | x^{(t-1)}, h^{(t-1)})$  that admits  $p_\theta(x)q_\phi(h|x)$  as the invariant distribution. There are many options. For continuous observations, SGLD (stochastic gradient Langevin dynamics) [36] and SGHMC (Stochastic Gradient Hamiltonian Monte Carlo) [3] sampling provide mechanisms for exploiting (stochastic) gradients of the target density, enabling more efficient exploration of the state space. [37] uses Langevin sampling without MH accept-reject, which is essentially SGLD. Intuitively, by choosing a decreasing sequence of discrete-time step-sizes (approaching zero), the discretization error incurred by SGLD/SGHMC will be negligible so that the MH rejection probability will approach zero and we may simply ignore this rejection step, and thus completely avoid the computation of the MH ratio. However, it is remains unclear whether this use of SGLD/SGHMC within the SA algorithm is theoretical sound.

In this paper, we propose to utilize SGHMC to exploit gradient information with momentum, which is found to perform better than SGLD. Furthermore, we provide a rigorous justification of this use of

---

<sup>7</sup>Such optimization using two objectives is employed in a number of familiar learning methods, such as GAN with logD trick, wake-sleep algorithm.

SGLD/SGHMC within the SA algorithm. The basic idea is to first take the theoretical results about SGLD from [32] and SGHMC from [3], which are briefly summarized in the following, and then extend the Markov state in SA to include the step-size used in SGLD/SGHMC.

**Theorem 1.** Denote the target density as  $p(z; \lambda)$  with given  $\lambda$ . Assume that one can compute a noisy, unbiased estimate  $\Delta(z, \xi; \lambda)$  to the gradient  $\frac{\partial}{\partial z} \log p(z; \lambda)$ , where  $\xi$  is an auxiliary random variable which contains all the randomness involved in constructing the estimate, namely  $E[\Delta(z, \xi; \lambda)] = \frac{\partial}{\partial z} \log p(z; \lambda)$ . Assume the stability Assumptions 4 in [32] holds.

For a sequence of asymptotically vanishing time-steps  $\{\delta_m, m \geq 1\}$  (satisfying  $\sum_{m=1}^{\infty} \delta_m = \infty$  and  $\sum_{m=1}^{\infty} \delta_m^2 < \infty$ ), an i.i.d. sequence  $\eta^{(m)}$ , and an independent and i.i.d. sequence  $\xi_m$  of auxiliary random variables,  $m \geq 1$ , the SGLD iterates as follows, starting from  $z^{(0)}$ :

$$z^{(m)} = z^{(m-1)} + \frac{\delta_m}{2} \Delta(z^{(m-1)}, \xi_m; \lambda) + \sqrt{\delta_m} \eta^{(m)}, \eta^{(m)} \sim \mathcal{N}(0, I), m = 1, \dots \quad (6)$$

Starting from  $z^{(0)}$  and  $v^{(0)} = 0$ , the SGHMC iterates as follows:

$$\begin{cases} v^{(m)} = \beta v^{(m-1)} + \frac{\delta_m}{2} \Delta(z^{(m-1)}, \xi_m; \lambda) + \sqrt{\delta_m} \eta^{(m)}, \eta^{(m)} \sim \mathcal{N}(0, I) \\ z^{(m)} = z^{(m-1)} + v^{(m)}, m = 1, \dots \end{cases} \quad (7)$$

Then in both cases, the non-homogeneous Markov chain  $\{z^{(m)}, m \geq 1\}$  converges to the equilibrium distribution  $p(z; \lambda)$ .

To plug finite steps of SGLD/SGHMC iterations in the SA algorithm, we introduce a Markov chain with  $\{0\} \cup \{\delta_m, m \geq 1\}$  as the state space. The Markov transitions are from  $\delta_m$  to  $\delta_{m+1}$  with probability one ( $m = 1, \dots$ ), and 0 is the absorbing state. Then, we consider an extended state  $(z, \delta)$  with the joint distribution  $p(z; \lambda)1(\delta = 0)$ , where  $1(\delta = 0)$  represents the single-point distribution. Then the Markov transition defined by Eq.(6)/(7) together with the above Markov transition defined over time-steps give a valid (homogeneous) Markov transition kernel that admits  $p(z; \lambda)1(\delta = 0)$  as the invariant distribution, according to Theorem 1. In this way, we equivalently transform non-homogeneous Markov transitions into homogeneous, and the condition to apply the SA algorithm is faithfully satisfied.

Finally, we can obtain the following construction of the Markov kernel that admits  $p_{\theta}(x)q_{\phi}(h|x)$  as the invariant distribution, by letting  $z \triangleq (x, h)$ ,  $p(z; \lambda) \triangleq p_{\theta}(x)q_{\phi}(h|x)$ ,  $\lambda \triangleq (\theta, \phi)^T$  in Theorem 1.

1. Do ancestral sampling by the generator, namely first drawing  $h' \sim p(h')$ , and then drawing  $x' \sim q_{\phi}(x'|h')$ ;
2. Starting from  $(x', h') = z^{(0)}$ , execute *sample revision* by running finite steps of SGLD/SGHMC ( $m = 1, \dots, M$ ) to obtain  $(x, h) = z^{(M)}$ , according to Eq.(6)/(7).

In sample revision, the calculation of the gradient,  $\frac{\partial}{\partial h} \log p(z; \lambda) = \frac{\partial}{\partial h} \log q_{\phi}(h, x)$ , is straightforward. For the gradient w.r.t.  $x$ , we have

$$\frac{\partial}{\partial x} \log p(z; \lambda) = \frac{\partial}{\partial x} \log p_{\theta}(x) + \frac{\partial}{\partial x} \log q_{\phi}(h, x) - \frac{\partial}{\partial x} \log q_{\phi}(x). \quad (8)$$

where the last term can be approximated by an unbiased estimate, as proved in the Supplement:

$$\frac{\partial}{\partial x} \log q_{\phi}(x) \approx \frac{\partial}{\partial x} \log q_{\phi}(h, x).$$

Therefore, we can use  $\frac{\partial}{\partial x} \log p_{\theta}(x)$ <sup>8</sup> as an unbiased estimate of the gradient  $\frac{\partial}{\partial x} \log p(z; \lambda)$ , and we can apply Theorem 1 with tractable gradients.

Intuitively, the generator gives a proposal  $(x', h')$ , and then the system follows the gradients of  $p_{\theta}(x)$  and  $q_{\phi}(h, x)$  (w.r.t.  $x$  and  $h$  respectively) to revise  $(x', h')$  to  $(x, h)$ . The gradient terms pull samples moving to low energy region of the random field and adjust the latent code of the generator, while the noise term brings randomness. Combining the above analysis, we can ignore the MH rejection step and accept  $(x, h)$  as samples from  $p_{\theta}(x)q_{\phi}(h|x)$ .

<sup>8</sup>Note that  $\frac{\partial}{\partial x} \log p_{\theta}(x) = \frac{\partial}{\partial x} u_{\theta}(x)$  does not need the calculation of the normalizing constant.

### 3.3 Semi-supervised learning

In semi-supervised tasks, we consider a RF for joint modeling of observation  $x$  and class label  $y$

$$p_\theta(x, y) = \frac{1}{Z(\theta)} \exp [u_\theta(x, y)] \quad (9)$$

which is different from Eq.2 for unsupervised learning without labels. The potential function  $u_\theta(x, y)$  is implemented by a neural network with  $x$  as the input and the output size is equal to the number of class labels. Denote by  $\Phi_\theta(x)$  the feature vector extracted by the neural network from the input  $x$ . Then we have  $u_\theta(x, y) = \text{onehot}(y)^T \Phi_\theta(x)$ , where  $\text{onehot}(y)$  represents the one-hot encoding vector for the label  $y$ . In this manner,  $p_\theta(y|x)$  is the classifier, defined as follows:

$$p_\theta(y|x) = \frac{p_\theta(x, y)}{p_\theta(x)} = \frac{\exp [u_\theta(x, y)]}{\sum_y \exp [u_\theta(x, y)]} \quad (10)$$

which acts like multi-class logistic regression using features  $\Phi_\theta(x)$  calculated from  $x$  by the neural network, and we do not need to calculate  $Z(\theta)$  for classification. The auxiliary generator is implemented the same as in Eq.3.

Suppose that among the data  $\mathcal{D} = \{\tilde{x}_1, \dots, \tilde{x}_n\}$ , only a small subset of the observations, for example the first  $m$  observations, have class labels,  $m \ll n$ . Denote these labeled data as  $\mathcal{L} = \{(\tilde{x}_1, \tilde{y}_1), \dots, (\tilde{x}_m, \tilde{y}_m)\}$ . Then we can formulate the semi-supervised learning as jointly optimizing

$$\begin{cases} \min_\theta KL [\tilde{p}(\tilde{x}) || p_\theta(\tilde{x})] - \alpha_d \sum_{(\tilde{x}, \tilde{y}) \sim \mathcal{L}} \log p_\theta(\tilde{y}|\tilde{x}) \\ \min_\phi KL [p_\theta(x) || q_\phi(x)] \end{cases} \quad (11)$$

which are defined by hybrids of generative and discriminative criteria, similar to [39, 16]. The hyper-parameter  $\alpha_d$  controls the relative weight between generative and discriminative criteria. By setting the gradients to zeros, the above optimization problem can be solved by finding the root for the following system of simultaneous equations:

$$\begin{cases} E_{\tilde{p}(\tilde{x})} \left[ \frac{\partial}{\partial \theta} \log p_\theta(\tilde{x}) \right] + \alpha_d \sum_{(\tilde{x}, \tilde{y}) \sim \mathcal{L}} \frac{\partial}{\partial \theta} \log p_\theta(\tilde{y}|\tilde{x}) \\ = E_{\tilde{p}(\tilde{x})} \left[ \frac{\partial}{\partial \theta} u_\theta(\tilde{x}) \right] - E_{p_\theta(x)} \left[ \frac{\partial}{\partial \theta} u_\theta(x) \right] + \alpha_d \sum_{(\tilde{x}, \tilde{y}) \sim \mathcal{L}} \frac{\partial}{\partial \theta} \log p_\theta(\tilde{y}|\tilde{x}) = 0 \\ E_{p_\theta(x)} \left[ \frac{\partial}{\partial \phi} \log q_\phi(x) \right] = E_{p_\theta(x)q_\phi(h|x)} \left[ \frac{\partial}{\partial \phi} \log q_\phi(x, h) \right] = 0 \end{cases} \quad (12)$$

where, with abuse of notation,

$$u_\theta(x) \triangleq \log \sum_y \exp [u_\theta(x, y)] \quad (13)$$

is the potential function for the marginal density  $p_\theta(x)$ , since we have  $p_\theta(x) = \frac{1}{Z(\theta)} \exp [u_\theta(x)]$  according to Eq.9. Similarly, it can be shown that Eq.(12) exactly follows the form of Eq.(1), so that we can apply the SA algorithm to find its root and thus solve the optimization problem Eq.(11). The SA algorithm with multiple moves for SSL is shown in Algorithm 3 in the Supplement. Apart from the basic losses as shown in Eq.(11), there are some regularization losses that are helpful to guide SSL learning and are presented in the Supplement.

## 4 Experiments

We conduct a series of experiments to study the performance of our method (NRF-IAGs) and various existing methods on synthetic and real-world datasets for both unsupervised and semi-supervised learning tasks, with both visual and numerical evaluation. We refer to the Supplement for experimental details and additional results.

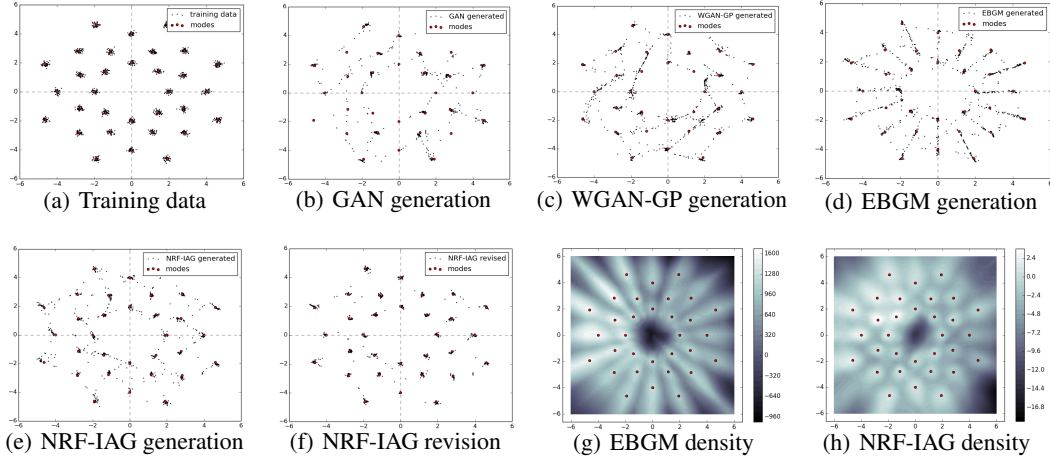


Figure 1: Comparison of different methods over GMM synthetic data. Stochastic generations from GAN (using logD trick), WGAN-GP, EBGM, NRF-IAG generation (i.e. sampling from the auxiliary generator) and NRF-IAG revision (i.e. after sample revision), are shown in (b)-(f) respectively. The red dots represent the modes of the data density. Each generation contains 1,000 samples. The learned densities ( $u_\theta(x)$ ) from EBGM and NRF-IAG are shown in (g) and (h) respectively.

Table 1: Numerical evaluations with GMM (32 components) synthetic data. The “covered modes” metric is defined as the number of covered modes by a set of generated samples. The “realistic ratio” metric is defined as the proportion of generated samples which are close to a mode. The measurement details are presented in the Supplement. Mean and SD are from 10 independent runs.

Methods	covered modes	realistic ratio
GAN	$22.25 \pm 1.54$	$0.90 \pm 0.01$
WGAN-GP	$27.81 \pm 1.40$	$0.74 \pm 0.04$
EBGM	$28.14 \pm 0.68$	$0.73 \pm 0.03$
NRF-IAG generation	$29.52 \pm 0.54$	$0.84 \pm 0.01$
NRF-IAG revision	$30.75 \pm 0.43$	$0.97 \pm 0.01$

Table 2: Inception scores (IS) on CIFAR-10 for unsupervised learning. Results with ResNets are not included. “ $^\dagger$ ” is reported in [2]. Mean and SD are from 10 independent runs.

Methods	CIFAR-10 IS
DCGAN $^\dagger$ [25]	$6.16 \pm 0.07$
WGAN-GP $^\dagger$ [10]	$6.56 \pm 0.05$
Improved-GAN [29]	$4.36 \pm 0.04$
ALI [8]	$5.34 \pm 0.05$
D2GAN [24]	$7.15 \pm 0.07$
DFM [35]	$7.72 \pm 0.13$
NRF-IAG with SGLD	$7.07 \pm 0.12$
NRF-IAG with SGHMC	$7.18 \pm 0.10$

#### 4.1 GMM synthetic data

The synthetic data consist of 1,600 training examples generated from a 2D Gaussian mixture model (GMM) with 32 equally-weighted, low-variance ( $\sigma = 0.1$ ) Gaussian components, uniformly laid out on four concentric circles as in Figure 1(a). The data distribution exhibits many modes separated by large low-probability regions, which makes it suitable to examine how well different learning methods can deal with multiple modes. For comparison, we experiment with GAN [9] (using logD trick) and WGAN-GP [10] for directed generative model, EBGM [11] and NRF-IAG for undirected generative model. We use SGLD for NRF-IAG on this synthetic dataset.

Figure 1 visually shows the generated samples from the trained models using different methods. Tab.1 reports the “covered modes” and “realistic ratio” as numerical measures of how the multi-modal data are fitted, similarly as in [8]. The main observations are as follows. First, GAN suffers from mode missing, generating realistic but not diverse samples. WGAN-GP increases “covered modes” but decreases “realistic ratio”. NRF-IAG performs better than both GAN and WGAN-GP in sample generation. Second, NRF-IAG outperforms EBGM in both sample generation and density estimation. Third, after revision, samples from NRF-IAG become more like samples from real data, achieving the best in both “covered modes” and “realistic ratio” metrics.

Table 3: Comparison with state-of-the-art methods on three benchmark datasets. “CIFAR-10 IS” means the inception score of samples generated by models trained for SSL on CIFAR-10. “ $\dagger$ ” is obtained by running the released code accompanied by the corresponding papers. “-” means the results are not reported and without released code. “\*” means these models cannot generate samples stochastically. “ $\ddagger$ ” uses image data augmentation which significantly helps classification performance. The upper/lower block show generative/discriminative SSL methods respectively.

Methods	MNIST (# error)	SVHN (% error)	CIFAR-10 (% error)	CIFAR-10 IS
CatGAN [30]	$191 \pm 10$	-	$19.58 \pm 0.46$	$3.57 \pm 0.13^\dagger$
SDGM [19]	$132 \pm 7$	$16.61 \pm 0.24$	-	-
Ladder network[26]	$106 \pm 37$	-	$20.40 \pm 0.47$	*
ADGM [19]	$96 \pm 2$	22.86	-	-
Improved-GAN [29]	$93 \pm 6.5$	$8.11 \pm 1.3$	$18.63 \pm 2.32$	$3.87 \pm 0.03$
ALI [8]	-	$7.42 \pm 0.65$	$17.99 \pm 1.62$	-
Triple-GAN[4]	$91 \pm 58$	$5.77 \pm 0.17$	$16.99 \pm 0.36$	$5.08 \pm 0.09$
BadGAN [7]	$79.5 \pm 9.8$	$4.25 \pm 0.03$	$14.41 \pm 0.30$	$3.46 \pm 0.11^\dagger$
<b>semi-NRF-IAGs</b>	$97 \pm 10$	$5.84 \pm 0.15$	$15.51 \pm 0.36$	$7.35 \pm 0.09$
VAT small [20]	136	6.83	14.87	*
$\Pi$ model $^\ddagger$ [15]	-	$4.82 \pm 0.17$	$12.36 \pm 0.31$	*
Temporal Ensembling $^\ddagger$ [15]	-	$4.42 \pm 0.16$	$12.16 \pm 0.31$	*
Mean Teacher $^\ddagger$ [31]	-	$3.95 \pm 0.19$	$12.31 \pm 0.28$	*
VAT+EntMin $^\ddagger$ [20]	-	3.86	10.55	*

## 4.2 Unsupervised learning on CIFAR-10

We examine unsupervised learning over the widely used real-world dataset CIFAR-10 [14]. To evaluate sample quality quantitatively, we use inception score [29], which takes into account that the samples are both diverse and realistic and is usually consistent with human judgment. Table 2 reports the inception scores for various methods, which are calculated using a widely used classification model from [29]. See the Supplement for generated samples, experimental details. We also show in the Supplement the capability of NRF-IAGs in latent space interpolation and conditional generation.

It can be seen from Table 2 that NRF-IAGs outperforms DCGAN [25], WGAN-GP [10], ALI [8], Improved-GAN [29] with a large margin, and performs slightly better than D2GAN [24] (3 networks). The higher IS from DFM [35] uses more complicated structure (3 networks) than NRF-IAGs (2 networks). In Table 2 and Figure S1(c)(d), we compare the performances of NRF-IAGs with SGLD and SGHMC. Utilizing SGHMC in NRF-IAGs to exploit gradient information with momentum yields better performance than simple SGLD as used in [37].

## 4.3 Semi-supervised learning results

For semi-supervised learning, we consider three widely used benchmark datasets, namely MNIST [18], SVHN [22], and CIFAR-10 [14]. As in previous work, we randomly sample 100, 1,000, and 4,000 labeled samples for MNIST, SVHN, and CIFAR-10 respectively during training, and use the standard data split for testing. We use SGHMC for semi-NRF-IAGs for all three datasets.

It can be seen from Table 3 that semi-NRF-IAGs produce strong classification results comparable to state-of-art DGM-based SSL methods. Compared to triple-GANs, semi-NRF-IAGs outperform with a large margin on the more challenging CIFAR-10, while the error rates on MNIST and SVHN are close. Bad-GANs achieve better classification results, but as indicated by the low inception score, their generation is much worse than semi-NRF-IAGs. In fact, among DGM-based SSL methods, semi-NRF-IAGs achieve the best performance in sample generation. See Figure S1(a)(b) in the Supplement for generated samples. This is in contrast to the conflict of good classification and good generation, as observed in GAN-based SSL [29, 7]. It is analyzed in [7] that good GAN-based SSL requires a bad generator<sup>9</sup>. This is embarrassing and in fact obviates the original idea of generative

<sup>9</sup>This analysis is based on using the  $(K + 1)$ -class GAN-like discriminator objective for SSL. To the best of our knowledge, the conflict does not seem to be reported in previous generative SSL methods [39, 16] which use the  $K$ -class classifier like in semi-NRF-IAGs.

SSL - successful generative training, which indicates good generation, provides regularization for finding good classifiers [39, 16]<sup>10</sup>.

Finally, note that discriminative SSL method, such as VAT [20], temporal ensembling [15] and mean teacher [31], also produce superior performances, by utilizing data augmentation and consistency regularization. However, these methods are unable to generate (realistic) samples. It can be seen that discriminative SSL methods utilize different regularization from generative SSL methods. Their combination, as an interesting future work, could yield further performance improvement.

## 5 Discussion and Conclusion

In this paper we develop Neural Random Field learning with Inclusive-divergence minimized Auxiliary Generators (NRF-IAG), which is under-appreciated in the literature. We provide rigorous theoretical development in the SA framework and introduce SGHMC. Extensive empirical evaluations show that the new approach of learning NRF-IAG achieves superior performances in both unsupervised learning and semi-supervised learning, competitive with state-of-the-art DGMs. Interesting future work will consider NRF-IAGs in sequential and trans-dimensional data modeling tasks.

The superior performances presumably are attributed to the two distinctive features in NRF-IAG learning - optimizing the inclusive KL for the auxiliary generator, and utilizing sample revision by SGLD/SGHMC. The auxiliary generator learned by inclusive KL tends to cover modes of the target density  $p_\theta$ , and sample revision pushes the samples towards the modes of  $p_\theta$ . This helps to produce Markov chains that mix faster between modes and thus facilitate model learning, which might explain NRF-IAGs' superior performances. In contrast, optimizing the exclusive KL, e.g. in [11], enforces the generator to seek modes and there is no sample revision; and the intractable entropy term further cause much difficulty in model learning.

---

<sup>10</sup>In this sense, Bad-GANs could hardly be classified as a generative SSL method.

## References

- [1] C. Andrieu, É. Moulines, and P. Priouret. Stability of stochastic approximation under verifiable conditions. *SIAM Journal on control and optimization*, 44(1):283–312, 2005.
- [2] L. Chen, S. Dai, Y. Pu, E. Zhou, C. Li, Q. Su, C. Chen, and L. Carin. Symmetric variational autoencoder and connections to adversarial learning. In *AISTATS*, 2018.
- [3] T. Chen, E. Fox, and C. Guestrin. Stochastic gradient hamiltonian monte carlo. In *ICML*, 2014.
- [4] L. Chongxuan, T. Xu, J. Zhu, and B. Zhang. Triple generative adversarial nets. In *NIPS*, 2017.
- [5] J. Dai, Y. Lu, and Y.-N. Wu. Generative modeling of convolutional neural networks. *arXiv preprint arXiv:1412.6296*, 2014.
- [6] Z. Dai, A. Almahairi, P. Bachman, E. Hovy, and A. Courville. Calibrating energy-based generative adversarial networks. In *ICLR*, 2017.
- [7] Z. Dai, Z. Yang, F. Yang, W. W. Cohen, and R. R. Salakhutdinov. Good semi-supervised learning that requires a bad gan. In *NIPS*, 2017.
- [8] V. Dumoulin, I. Belghazi, B. Poole, O. Mastropietro, A. Lamb, M. Arjovsky, and A. Courville. Adversarially learned inference. In *ICLR*, 2017.
- [9] I. J. Goodfellow, J. Pouget-Abadie, M. Mirza, B. Xu, D. Warde-Farley, S. Ozair, A. Courville, and Y. Bengio. Generative adversarial nets. In *NIPS*, 2014.
- [10] I. Gulrajani, F. Ahmed, M. Arjovsky, V. Dumoulin, and A. C. Courville. Improved training of wasserstein gans. In *NIPS*, 2017.
- [11] T. Kim and Y. Bengio. Deep directed generative models with energy-based probability estimation. *arXiv preprint arXiv:1606.03439*, 2016.
- [12] D. P. Kingma and M. Welling. Auto-encoding variational bayes. In *ICLR*, 2014.
- [13] D. Koller and N. Friedman. *Probabilistic graphical models: principles and techniques*. MIT press, 2009.
- [14] A. Krizhevsky. Learning multiple layers of features from tiny images. *Technical report, University of Toronto*, 2009.
- [15] S. Laine and T. Aila. Temporal ensembling for semi-supervised learning. In *ICLR*, 2017.
- [16] H. Larochelle, M. Mandel, R. Pascanu, and Y. Bengio. Learning algorithms for the classification restricted boltzmann machine. *JMLR*, 13(1):643–669, 2012.
- [17] Y. LeCun, S. Chopra, and R. Hadsell. A tutorial on energy-based learning. *Predicting Structured Data*, 2006.
- [18] Y. Lécun, L. Bottou, Y. Bengio, and P. Haffner. Gradient-based learning applied to document recognition. *Proceedings of the IEEE*, 86(11):2278–2324, 1998.
- [19] L. Maaløe, C. K. Sønderby, S. K. Sønderby, and O. Winther. Auxiliary deep generative models. In *ICML*, 2016.
- [20] T. Miyato, S.-i. Maeda, M. Koyama, and S. Ishii. Virtual adversarial training: a regularization method for supervised and semi-supervised learning. *arXiv preprint arXiv:1704.03976*, 2017.
- [21] R. M. Neal et al. Mcmc using hamiltonian dynamics. *Handbook of Markov Chain Monte Carlo*, 2011.
- [22] Y. Netzer, T. Wang, A. Coates, A. Bissacco, B. Wu, and A. Y. Ng. Reading digits in natural images with unsupervised feature learning. In *NIPS Workshop on Deep Learning and Unsupervised Feature Learning*, 2012.
- [23] J. Ngiam, Z. Chen, W. K. Pang, and A. Y. Ng. Learning deep energy models. In *ICML*, 2012.
- [24] T. Nguyen, T. Le, H. Vu, and D. Phung. Dual discriminator generative adversarial nets. In *NIPS*. 2017.
- [25] A. Radford, L. Metz, and S. Chintala. Unsupervised representation learning with deep convolutional generative adversarial networks. *arXiv preprint arXiv:1511.06434*, 2015.

- [26] A. Rasmus, M. Berglund, M. Honkala, H. Valpola, and T. Raiko. Semi-supervised learning with ladder networks. In *NIPS*, 2015.
- [27] H. Robbins and S. Monro. A stochastic approximation method. *The Annals of Mathematical Statistics*, 1951.
- [28] R. Salakhutdinov and G. Hinton. Deep boltzmann machines. *JMLR*, 2009.
- [29] T. Salimans, I. Goodfellow, W. Zaremba, V. Cheung, A. Radford, and X. Chen. Improved techniques for training gans. In *NIPS*, 2016.
- [30] J. T. Springenberg. Unsupervised and semi-supervised learning with categorical generative adversarial networks. *arXiv preprint arXiv:1511.06390*, 2015.
- [31] A. Tarvainen and H. Valpola. Mean teachers are better role models: Weight-averaged consistency targets improve semi-supervised deep learning results. In *NIPS*, 2017.
- [32] Y. W. Teh, A. H. Thiery, and S. J. Vollmer. Consistency and fluctuations for stochastic gradient langevin dynamics. *JMLR*, 2016.
- [33] B. Wang and Z. Ou. Language modeling with neural trans-dimensional random fields. In *IEEE Automatic Speech Recognition and Understanding Workshop*, pages 294–300, 2017.
- [34] B. Wang, Z. Ou, and Z. Tan. Learning trans-dimensional random fields with applications to language modeling. *IEEE Transactions on Pattern Analysis and Machine Intelligence*, 2018.
- [35] D. Warde-Farley and Y. Bengio. Improving generative adversarial networks with denoising feature matching. In *ICLR*, 2017.
- [36] M. Welling and Y. W. Teh. Bayesian learning via stochastic gradient langevin dynamics. In *ICML*, 2011.
- [37] J. Xie, Y. Lu, S.-C. Zhu, and Y. N. Wu. Cooperative training of descriptor and generator networks. *arXiv preprint arXiv:1609.09408*, 2016.
- [38] J. Zhao, M. Mathieu, and Y. Lecun. Energy-based generative adversarial network. In *ICLR*, 2017.
- [39] X. Zhu. Semi-supervised learning literature survey. *Technical Report 1530, University of Wisconsin Madison*, 2005.

---

# Supplement for “Learning Neural Random Fields with Inclusive Auxiliary Generators”

---

**Yunfu Song, Zhijian Ou**  
Tsinghua University, Beijing, China  
ozj@tsinghua.edu.cn

## 1 Convergence of the SA Algorithm 1

For completeness, we provide a short summary on the convergence of  $\{\lambda_t, t \geq 1\}$  in Algorithm 1, based on Theorem 5.5 in [1].

**Theorem 2.** *Let  $\{\gamma_t\}$  be a monotone nonincreasing sequence of positive numbers such that<sup>11</sup>  $\sum_{t=1}^{\infty} \gamma_t = \infty$  and  $\sum_{t=1}^{\infty} \gamma_t^2 < \infty$ . Assume that  $\Lambda$  is compact and the Lyapunov condition on  $f(\lambda)$  and the drift condition on the transition kernel  $K_{\lambda}(\cdot, \cdot)$  hold. Then we have:  $d(\lambda_t, \mathcal{L}) \rightarrow 0$  almost surely as  $t \rightarrow \infty$ , where  $\mathcal{L} = \{\lambda : f(\lambda) = 0\}$  and  $d(\lambda, \mathcal{L}) = \inf_{\lambda' \in \mathcal{L}} \|\lambda - \lambda'\|$ .*

## 2 Unbiased gradient estimate in applying SGLD/SGHMC

**Proposition 2.** *Let  $z \triangleq (x, h)$ ,  $p(z; \lambda) \triangleq p_{\theta}(x)q_{\phi}(h|x)$ ,  $\lambda \triangleq (\theta, \phi)^T$  in Theorem 1. The initial value  $(x^{(0)}, h^{(0)})$  is obtained from ancestral sampling by the generator. The SGLD/SGHMC as shown in Eq.(6)/(7) iteratively generates  $(x^{(m)}, h^{(m)})$ ,  $m = 1, \dots$ . Then,  $\frac{\partial}{\partial x^{(m)}} \log q_{\phi}(h^{(m)}, x^{(m)})$  is an unbiased estimate of the gradient  $\frac{\partial}{\partial x^{(m)}} \log q_{\phi}(x^{(m)})$ ,  $m = 0, 1, \dots$*

*Proof.* Note that Langevin dynamics and Hamiltonian dynamics are reversible [21]. Thus the SGLD/SGHMC transitions Eq.(6)/(7) satisfy the detailed balance condition:

$\pi(h^{(m-1)}, x^{(m-1)})K(h^{(m)}, x^{(m)}|h^{(m-1)}, x^{(m-1)}) = \pi(h^{(m)}, x^{(m)})K(h^{(m-1)}, x^{(m-1)}|h^{(m)}, x^{(m)})$ , where  $\pi(\cdot)$  denotes the target density, and  $K(\cdot|\cdot)$  denotes the transition kernel. Also note that  $E_{h \sim q_{\phi}(h|x)} \left[ \frac{\partial}{\partial x} \log q_{\phi}(h, x) \right] = \frac{\partial}{\partial x} \log q_{\phi}(x)$ . Thus if we show that  $h^{(m)}$  is indeed drawn from  $q_{\phi}(h^{(m)}|x^{(m)})$  during sample revision,  $m = 0, 1, \dots$ , then the unbiasedness will hold.

Denote by  $\pi^{(m)}(h^{(m)}, x^{(m)})$  the state-occupation density at step  $m$ . Then we need to show that  $\pi^{(m)}(h^{(m)}|x^{(m)})$  actually follows  $\pi(h^{(m)}|x^{(m)})$ , i.e.  $q_{\phi}(h^{(m)}|x^{(m)})$ ,  $m = 0, 1, \dots$ .

First, it is obvious that this holds for  $(h^{(0)}, x^{(0)})$ . Then, we proceed by mathematical induction. Suppose  $\pi^{(m-1)}(h^{(m-1)}|x^{(m-1)}) = \pi(h^{(m-1)}|x^{(m-1)})$ . Then we have

$$\begin{aligned} & \pi^{(m-1)}(h^{(m-1)}, x^{(m-1)})K(h^{(m)}, x^{(m)}|h^{(m-1)}, x^{(m-1)}) \\ &= \pi^{(m-1)}(h^{(m-1)}, x^{(m-1)}) \frac{\pi(h^{(m)}, x^{(m)})}{\pi(h^{(m-1)}, x^{(m-1)})} K(h^{(m-1)}, x^{(m-1)}|h^{(m)}, x^{(m)}). \end{aligned} \quad (\text{S1})$$

Integrating out  $(h^{(m-1)}, x^{(m-1)})$  from both sides of Eq.S1, we obtain

$$\begin{aligned} \pi^{(m)}(h^{(m)}, x^{(m)}) &= \pi(h^{(m)}, x^{(m)}) \sum_{x^{(m-1)}} \frac{\pi^{(m-1)}(x^{(m-1)})}{\pi(x^{(m-1)})} K(x^{(m-1)}|h^{(m)}, x^{(m)}) \\ &= \pi(h^{(m)}, x^{(m)}) \sum_{x^{(m-1)}} \frac{\pi^{(m-1)}(x^{(m-1)})}{\pi(x^{(m-1)})} K(x^{(m-1)}|x^{(m)}) \end{aligned}$$

<sup>11</sup>In practice, we can set a large learning rate at the early stage of learning and decrease to  $1/t$  for convergence.

where the second equality, i.e.  $K(x|h', x') = K(x|x')$ , holds because in the SGLD/SGHMC transitions Eq.(6)/(7), generating next step  $x$  only depends on current  $x'$  and is independent of current  $h'$ . Then we have

$$\begin{aligned}\pi^{(m)}(h^{(m)}|x^{(m)}) &= \pi(h^{(m)}|x^{(m)}) \frac{\pi(x^{(m)})}{\pi^{(m)}(x^{(m)})} \sum_{x^{(m-1)}} \frac{\pi^{(m-1)}(x^{(m-1)})}{\pi(x^{(m-1)})} K(x^{(m-1)}|x^{(m)}) \\ &= \pi(h^{(m)}|x^{(m)})\end{aligned}$$

where the second equality holds because we have

$$\begin{aligned}& \frac{\pi(x^{(m)})}{\pi^{(m)}(x^{(m)})} \sum_{x^{(m-1)}} \frac{\pi^{(m-1)}(x^{(m-1)})}{\pi(x^{(m-1)})} K(x^{(m-1)}|x^{(m)}) \\ &= \frac{1}{\pi^{(m)}(x^{(m)})} \sum_{x^{(m-1)}} \pi^{(m-1)}(x^{(m-1)}) \frac{K(x^{(m-1)}|x^{(m)})\pi(x^{(m)})}{\pi(x^{(m-1)})} \\ &= 1\end{aligned}$$

Thereby, we show  $h^{(m)} \sim \pi(h^{(m)}|x^{(m)})$ , i.e.  $q_\phi(h^{(m)}|x^{(m)})$ . This concludes the inductive step.  $\square$

### 3 Semi-supervised learning

---

**Algorithm 3** Semi-supervised learning of neural RFs with inclusive auxiliary generators

---

**repeat**

Monte Carlo sampling:

Draw a unsupervised minibatch  $\mathcal{U} \sim \tilde{p}(\tilde{x})p_\theta(x)q_\phi(h|x)$  and a supervised minibatch  $\mathcal{S} \sim \mathcal{L}$ ;  
SA updating:

Update  $\theta$  by ascending:

$$\begin{aligned}& \frac{1}{|\mathcal{U}|} \sum_{(\tilde{x}, x, h) \sim \mathcal{U}} \left[ \frac{\partial}{\partial \theta} u_\theta(\tilde{x}) - \frac{\partial}{\partial \theta} u_\theta(x) \right] + \alpha_d \frac{1}{|\mathcal{S}|} \sum_{(\tilde{x}, \tilde{y}) \sim \mathcal{S}} \left[ \frac{\partial}{\partial \theta} \log p_\theta(\tilde{y}|\tilde{x}) \right] \\ & - \frac{1}{|\mathcal{U}|} \sum_{(\tilde{x}, x, h) \sim \mathcal{U}} \left[ \alpha_c \frac{\partial}{\partial \theta} H(p_\theta(y|\tilde{x})) + \alpha_p \frac{\partial}{\partial \theta} [u_\theta(\tilde{x})]^2 \right]\end{aligned}$$

Update  $\phi$  by ascending:

$$\frac{1}{|\mathcal{U}|} \sum_{(\tilde{x}, x, h) \sim \mathcal{U}} \frac{\partial}{\partial \phi} \log q_\phi(x, h)$$

**until** convergence

---

Apart from the basic losses, as shown in Eq.12, in applying NRF-IAGs in SSL, there are some regularization losses that are helpful to guide the semi-supervised learning.

**Confidence loss.** Similar to [30, 4], we add the minimization of the conditional entropy of  $p_\theta(y|\tilde{x})$  averaged over training data to the loss w.r.t.  $\theta$  (i.e. the first line in Eq.11) as follows:

$$L_c(\theta) = E_{\tilde{p}(\tilde{x})} [H(p_\theta(y|\tilde{x}))] = -E_{\tilde{p}(\tilde{x})} \left[ \sum_y p_\theta(y|\tilde{x}) \log p_\theta(y|\tilde{x}) \right]$$

In this manner, we encourage the classifier  $p_\theta(y|x)$  derived from the RF to make classifications confidently. In practice, we use stochastic gradients of  $L_c(\theta)$  over minibatches in optimizing  $\theta$ , as shown in Algorithm 3.

**Potential control loss.** For random fields, the data log-likelihood  $\log p_\theta(\tilde{x})$  is determined relatively by the potential value  $u_\theta(\tilde{x})$ . To avoid the potential values not to increase unreasonably, we could control the squared potential values, by minimizing:

$$L_p(\theta) = E_{\tilde{p}(\tilde{x})} [u_\theta(\tilde{x})]^2$$

In this manner, the potential values would be attracted to zeros. In practice, we use stochastic gradients of  $L_s(\theta)$  over minibatches in optimizing  $\theta$ , as shown in Algorithm 3.

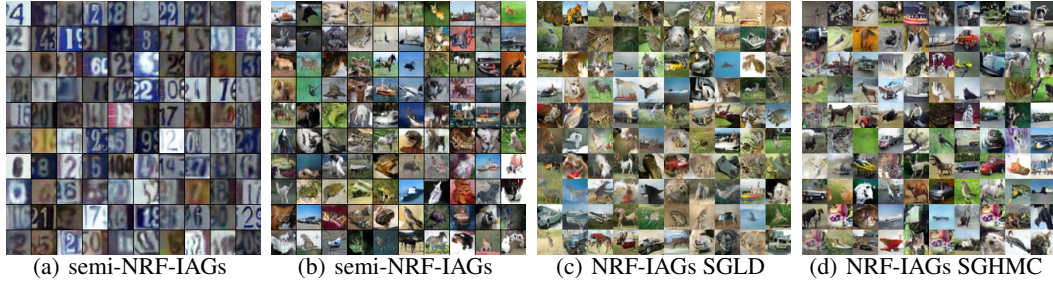


Figure S1: Generated samples from semi-NRF-IAGs (i.e. trained for SSL) on SVHN and CIFAR-10 are shown in (a) and (b) respectively. Generated samples from (unsupervised) NRF-IAGs on CIFAR-10 with SGLD and SGHMC are shown in (c) and (d) respectively.

## 4 Details of experiments

### 4.1 GMM synthetic data

In the GMM experiment, we use the following procedure to estimate the metrics “covered modes” and “realistic ratio” for each trained model.

1. Stochastically generate 100 samples.
2. A mode is defined to be covered (not missed) if there exist generated samples located closely to the mode (with squared distance  $< 0.02$ ), and those samples are said to be realistic.
3. Count how many modes are covered and calculate the proportion of realistic samples.
4. Repeat the above steps 100 times and perform averaging.

For each method, we independently train 10 models and calculate the mean and standard deviation (SD) across the 10 independent runs.

The network architectures and hyperparameters are the same for all methods, as listed in Table S1. We use SGLD [36] for NRF-IAGs on this synthetic dataset, with empirical revision hyperparameters  $\delta_m = 0.01$ .

### 4.2 NRF-IAGs (unsupervised) on CIFAR-10

The network architectures (taken from the released code by [25] and widely adopted by [10, 24, 35]) and hyperparameters for NRF-IAGs (unsupervised) on CIFAR-10, as listed in Table S2. For the use of SGLD and SGHMC [3] in sample revision for NRF-IAGs, we empirically choose the SGLD hyperparameters ( $\delta_m = 0.01$ ) and SGHMC hyperparameters ( $\beta = 0.5, \delta_m = 0.003$ ). Figure S1(c)(d) compare the generated samples from NRF-IAGs with SGLD and SGHMC.

### 4.3 semi-NRF-IAGs on MNIST, SVHN and CIFAR-10

The network architectures (taken from the released code by [29] and widely adopted by [4, 7]) and hyperparameters for semi-NRF-IAGs on MNIST, SVHN and CIFAR-10 are listed in Table S3, Table S4 and Table S5 respectively.

For semi-NRF-IAGs, we use SGHMC, with empirical revision hyperparameters ( $\beta = 0.5, \delta_m = 0.003$ ) for MNIST and CIFAR-10, and ( $\beta = 0.5, \delta_m = 0.01$ ) for SVHN. Figure S1(a)(b) show the generated samples from semi-NRF-IAGs trained over SVHN and CIFAR-10 respectively.

## 5 SSL toy experiment

In Figure S2, we present the performance of semi-NRF-IAGs for SSL on a synthetic dataset, which emphasizes that semi-NRF-IAGs can provide (unnormalized) density estimates for  $p_\theta(x)$ ,  $p_\theta(x, y = 1)$  and  $p_\theta(x, y = 2)$ . In contrast, the use of GANs as general purpose probabilistic generative models

has been limited by the difficulty in using them to provide density estimates or even unnormalized potential values for sample evaluation.

The dataset is a 2D GMM with 16 Gaussian components, uniformly laid out on two concentric circles. The two circles represent two different classes, each class with 4 labeled data and 400 unlabeled data. The network architectures are the same as S1, except that the neural network which implement the potential function  $u_\theta(x, y)$  for SSL now has two units in the output.

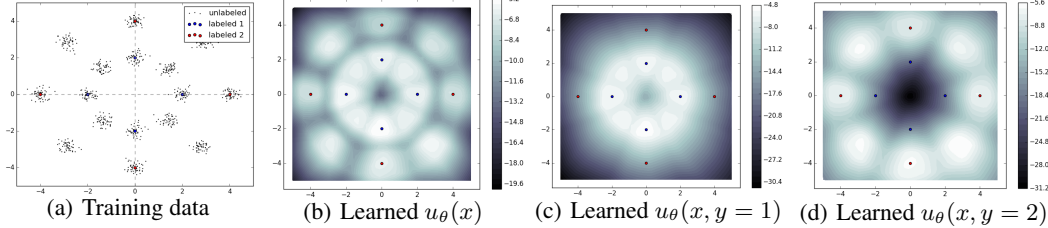


Figure S2: SSL toy experiment based on semi-NRF-IAGs. Each class has 4 labeled points, blue dots for class 1 and red for class 2. The learned potentials for  $u_\theta(x)$ ,  $u_\theta(x, y = 1)$  and  $u_\theta(x, y = 2)$  are shown in (b)(c)(d) respectively.

## 6 Latent space interpolation

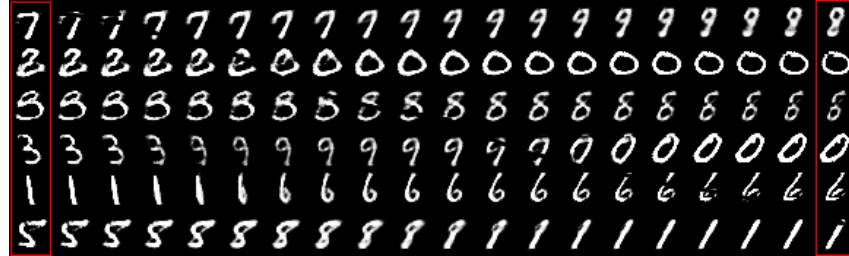


Figure S3: Latent space interpolation with NRF-IAGs on MNIST. The leftmost and rightmost columns are from stochastic generations  $x_1$  with latent code  $h_1$  and  $x_2$  with  $h_2$ . The columns in between correspond to the generations from the latent codes interpolated linearly from  $h_1$  to  $h_2$ .

Figure S3 shows that the auxiliary generator smoothly outputs transitional samples as the latent code  $h$  moves linearly in the latent space. The interpolated generation demonstrates that the model has indeed learned an abstract representation of the data.

## 7 Class-conditional generation

Figure S4 shows class-conditional generation results on MNIST with semi-NRF-IAGs. Notice that the generator does not explicitly include class labels, thus it is unable to perform class-conditional generation directly. However, the random field has modeling of  $p_\theta(x, y)$ , based on which we can perform class-conditional generation as follows:

1. Generate a sample  $x$  unconditionally, by ancestral sampling with the generator.
2. Predict the label  $y$  for the sample  $x$  by the random field;
3. Starting from  $x$ , running SGLD/SGHMC revision with  $p_\theta(x|y)$  as the target density by fixing  $y$ . The resulting samples could be viewed as conditional generations, according to Theorem 1.

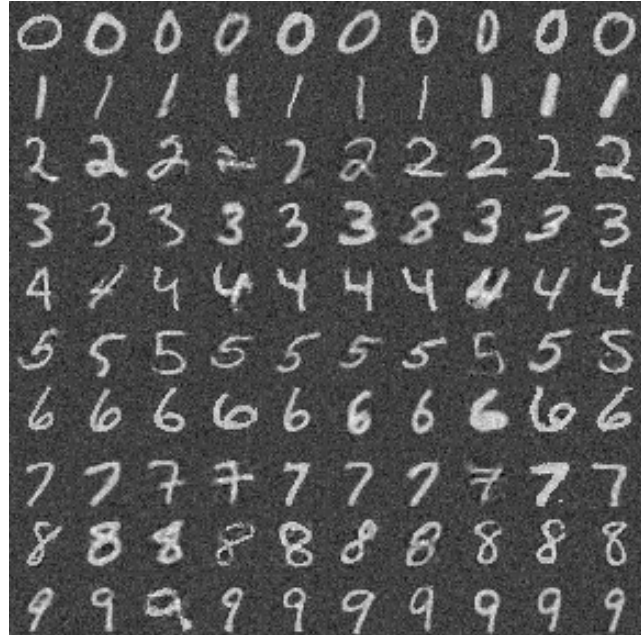


Figure S4: Conditional generated samples from semi-NRF-IAGs trained on MNIST. Due to sample revision, the background pixels are not purely black.

Table S1: Network architectures and hyperparameters for 2D GMM data.

Random Field	Generator
Input 2dims Colored Image	Noise $h$ (2dims)
MLP 100 units, Leaky ReLU	MLP 50 units, ReLU
MLP 100 units, Leaky ReLU	MLP 50 units, ReLU
MLP 1 unit, Linear	MLP 2 units, Linear
Batch size	100
Number of iterations	160,000
Leaky ReLU slope	0.2
Learning rate	0.001
Optimizer	Adam ( $\beta_1 = 0.5, \beta_2 = 0.9$ )
Sample revision steps	$M = 10$

Table S2: Network architectures and hyperparameters for NRF-IAGs (unsupervised) on CIFAR-10.

Random Field	Generator
Input $32 \times 32$ Colored Image	Noise $h$ (100dims)
$5 \times 5$ conv. 128, Stride=2, Leaky ReLU,	MLP 8192 units, ReLU, Batch norm
$5 \times 5$ conv. 256 Stride=2, Leaky ReLU, Batch norm	$5 \times 5$ deconv. 256, ReLU, Stride=2, Batch norm
$5 \times 5$ conv. 512 Stride=2, Leaky ReLU, Batch norm	$5 \times 5$ deconv. 128, ReLU, Stride=2, Batch norm
MLP 1 unit, Linear	$5 \times 5$ deconv. 3, Tanh, stride=2
Batch size	100
Number of epochs	400
Leaky ReLU slope	0.2
Learning rate	0.0002
Optimizer	Adam ( $\beta_1 = 0.5, \beta_2 = 0.9$ )
Sample revision steps	$M = 10$

Table S3: Network architectures and hyperparameters for semi-NRF-IAGs on MNIST

Random Field	Generator
Input $28 \times 28$ Gray Image	Noise $h$ (100dims)
MLP 1000 units, Leaky ReLU, Weight norm	MLP 500 units, Sotfplus, Batch norm
MLP 500 units, Leaky ReLU, Weight norm	MLP 500 units, Sotfplus, Batch norm
MLP 250 units, Leaky ReLU, Weight norm	MLP 784 units, Sigmoid
MLP 250 units, Leaky ReLU, Weight norm	
MLP 250 units, Leaky ReLU, Weight norm	
MLP 10 units, Linear, Weight norm	
Batch size	100
Number of epochs	200
Leaky ReLU slope	0.2
Learning rate	0.001
Optimizer	Adam ( $\beta_1 = 0.0, \beta_2 = 0.9$ )
Sample revision steps	$M = 20$
$\alpha$ in SSL	$\alpha_d = 10, \alpha_c = 10, \alpha_p = 0$

Table S4: Network architectures and hyperparameters for semi-NRF-IAGs on SVHN

Random Field	Generator
Input $32 \times 32$ Colored Image	Noise $h$ (100dims)
$3 \times 3$ conv. 64, Leaky ReLU, Weight norm	MLP 8192 units, ReLU, Batch norm
$3 \times 3$ conv. 64, Leaky ReLU, Weight norm	Reshape $512 \times 4 \times 4$
$3 \times 3$ conv. 64, Leaky ReLU, Weight norm	$5 \times 5$ deconv. 256, ReLU, Stride=2
stride=2, dropout2d=0.5	$5 \times 5$ deconv. 128, ReLU, Stride=2
$3 \times 3$ conv. 128, Leaky ReLU, Weight norm	$5 \times 5$ deconv. 3, Tanh, Stride=2
$3 \times 3$ conv. 128, Leaky ReLU, Weight norm	
$3 \times 3$ conv. 128, Leaky ReLU, Weight norm	
stride=2, dropout2d=0.5	
$3 \times 3$ conv. 128, Leaky ReLU, Weight norm	
$1 \times 1$ conv. 128, Leaky ReLU, Weight norm	
$1 \times 1$ conv. 128, Leaky ReLU, Weight norm	
MLP 10 units, Linear, Weight norm	
Batch size	100
Number of epochs	400
Leaky ReLU slope	0.2
Learning rate	0.001
Optimizer	Adam ( $\beta_1 = 0.0, \beta_2 = 0.9$ )
Sample revision steps	$M = 10$
$\alpha$ in SSL	$\alpha_d = 10, \alpha_c = 10, \alpha_p = 0$

Table S5: Network architectures and hyperparameters for semi-NRF-IAGs on CIFAR-10

Random Field	Generator
Input $32 \times 32$ Colored Image	Noise $h$ (100dims)
$3 \times 3$ conv. 128, Leaky ReLU, Weight norm	MLP 8192 units, ReLU, batch norm
$3 \times 3$ conv. 128, Leaky ReLU, Weight norm	Reshape $512 \times 4 \times 4$
$3 \times 3$ conv. 128, Leaky ReLU, Weight norm stride=2, dropout2d=0.5	$5 \times 5$ deconv. 256, ReLU, Stride=2 $5 \times 5$ deconv. 128 ReLU, stride=2
$3 \times 3$ conv. 256, Leaky ReLU, Weight norm	$5 \times 5$ deconv. 3, Tanh, Stride=2
$3 \times 3$ conv. 256, Leaky ReLU, Weight norm	
$3 \times 3$ conv. 256, Leaky ReLU, Weight norm stride=2, dropout2d=0.5	
$3 \times 3$ conv. 512, Leaky ReLU, Weight norm	
$1 \times 1$ conv. 256, Leaky ReLU, Weight norm	
$1 \times 1$ conv. 128, Leaky ReLU, Weight norm	
MLP 10 units, Linear, Weight norm	
Batch size	100
Number of epochs	600
Leaky ReLU slope	0.2
Learning rate	0.001
Optimizer	Adam ( $\beta_1 = 0.0, \beta_2 = 0.9$ )
Sample revision steps	$M = 10$
$\alpha$ in SSL	$\alpha_d = 100, \alpha_c = 0, \alpha_p = 0.1$